A bloody interaction: Plasma proteomics reveals gilthead sea bream (Sparus aurata) impairment caused by Sparicotyle chrysophrii

Enrique Riera-Ferrer
Institute of Aquaculture Torre de la Sal (IATS, CSIC), Ribera de Cabanes
M. Carla Piazzon
Institute of Aquaculture Torre de la Sal (IATS, CSIC), Ribera de Cabanes
Raquel Del Pozo
Institute of Aquaculture Torre de la Sal (IATS, CSIC), Ribera de Cabanes
Oswaldo Palenzuela
Institute of Aquaculture Torre de la Sal (IATS, CSIC), Ribera de Cabanes
Itziar Estensoro (itziar.estensoro@csic.es)
Institute of Aquaculture Torre de la Sal (IATS, CSIC), Ribera de Cabanes
Ariadna Sitjà-Bobadilla
Institute of Aquaculture Torre de la Sal (IATS, CSIC), Ribera de Cabanes

Research Article

Keywords: Sparicotyle chrysophrii, proteomics, haemoglobin, blood, immune system, host-parasite interactions, cholesterol

Posted Date: June 29th, 2022

DOI: https://doi.org/10.21203/rs.3.rs-1776373/v1

Abstract

Background:

Sparicotylosis is an endemic parasitic disease across the Mediterranean Sea caused by the polyopisthocotylean monogenean *Sparicotyle chrysophrii*, which affects the gills of gilthead sea bream (GSB; *Sparus aurata*). Current disease-management, mitigation and treatment strategies are scarce against sparicotylosis. In order to successfully develop more efficient therapeutic strategies against this disease, understanding which molecular mechanisms and metabolic pathways are altered in the host is critical. This study aims to elucidate how *S. chrysophrii* infection modulates GSB physiological status and to identify the main altered biological processes through plasma proteomics.

Methods:

Experimental infections were conducted in a recirculating aquaculture system (RAS), exposing naïve recipient GSB (R; 70 g; N= 50) to effluent water from *S. chrysophrii*-infected GSB. An additional tank with unexposed naïve fish (C; 70 g; N=50) was maintained in parallel, with open water flow disconnected from the RAS. Haematological and infection parameters from sampled C and R fish were registered for 10 weeks.

Plasma samples from R fish were categorised into 3 different groups according to their infection intensity in the right-sided gill arches: low, medium and high (L: 1-25; M: 26-50; H: >50 worms, respectively). Five plasma samples of each category were selected, in addition to five C samples and underwent a SWATH-MS proteome analysis. Additional assays on haemoglobin, cholesterol and the lytic activity of the alternative complement pathway were performed to validate the proteome analysis findings.

Results:

The discriminant analysis of the plasma protein abundance revealed a clear separation into 3 groups (H, M/L and C). A pathway analysis was performed with the differentially quantified proteins, indicating that the parasitic infection mainly affected pathways related to haemostasis, the immune system and lipid metabolism and transport.

Twenty-two proteins significantly correlated with the infection intensity, highlighting apolipoproteins, globins and complement *c3*. Validation assays in blood and plasma (haemoglobin, cholesterol and lytic activity of alternative complement pathway) confirmed these correlations.

Conclusions:

Sparicotylosis profoundly alters the haemostasis, the innate immune system and the lipid metabolism and transport in GSB. This study gives a crucial global overview of the pathogenesis of sparicotylosis and highlights new targets for further research.

Background

Sparicotylosis is caused by the gill infection of the polyopisthocotylean monogenean parasite *Sparicotyle chrysophrii* (*fmr Microcotyle chrysophrii*; Microcotylidae). This parasite has a direct life cycle in which gravid adult specimens shed embryonated eggs into the water column from which motile ciliated larvae hatch after a couple of weeks. If any hosts are nearby, they will attach to their gill filaments giving rise to post-larvae, and subsequently to juveniles and adults [1, 2].This disease is endemic in the Mediterranean Sea, affecting several fish species of the *Sparidae* family [3–7], amongst which gilthead sea bream (*Sparus aurata*; GSB) stands out due to its commercial relevance in the Mediterranean aquaculture industry [8].

Sparicotylosis is associated with lethargy due to hypoxia, severe anaemia, and emaciation. Gill histopathological signs such as lamellar synechiae, clubbing and shortening, epithelial hyperplasia resulting in secondary lamellae fusion, and proliferation of chloride cells have been described [9, 10].

Disease management in on-growing offshore net pens is a complex matter. The high stocking densities, the proximity of the cages, the marine currents and the seeding of fingerlings without year-class separation or fallowing strategies create a perfect niche for amplification and dissemination of any pathogen. Current methods to control sparicotylosis rely on disinfectant bath treatments, net changing or cleaning [11], and nutraceutical formulation feedings [12].

For more than two decades, efforts have been made to widen the chemotherapeutic alternatives against *S. chrysophrii* [9, 12, 13], but only hydrogen peroxide and formalin baths, which present a narrow therapeutic index and several concerns [12, 14–17], remain as treatment options against sparicotylosis. The successful development of more efficient therapeutic strategies to control sparicotylosis critically relies on the knowledge of the molecular mechanisms and metabolic pathways, which are relevant in the host-parasite relationship. Thus far, few studies dealing with *S. chrysophrii* – GSB interactions have been published. [18] described the inhibition of the humoral response and activation of cellular components in GSB – *S. chrysophrii* long-term infections. Later, a tissue-level transcriptomic analysis of mild *S. chrysophrii* infections revealed that apoptosis, inflammation and cell proliferation had leading roles in gills, whereas a hypometabolic response was detected in the spleen [19].

In recent years, proteomic analyses have transformed how host-parasite interactions are studied and understood. These interactions can be studied either by determining the expression of the parasite proteome throughout the infection (*i.e.*, tegumental and secreted proteins and extracellular vesicles), by detecting parasite proteins in its host, or by defining the infection effects on the host's proteome. Thus far, significant progress has been achieved in understanding critical high-impact zoonotic and animal parasitic diseases through this technology [20–29].

This study aims to elucidate how *S. chrysophrii* infection modulates GSB physiological status and to identify the main altered biological processes through plasma proteomics.

Methods

Animals, experimental infections and samplings

Healthy gilthead sea bream juveniles were purchased from a Mediterranean-based hatchery (Piscimar, Burriana, Spain) and adapted to the IATS-CSIC indoor experimental facilities under natural photoperiod and temperature conditions (40°5'N; 0°10'E). Water parameters were monitored; oxygen saturation was kept above 85% and unionised ammonia below 0.02 mg L^{-1} in all tanks.

The experimental infection was conducted in a recirculation aquaculture system (RAS). The experimental design consisted of a recipient (R) tank (200 L) holding naïve GSB (70 g; N = 50) receiving water from a donor (D) tank (200 L) with *Sparicotyle chrysophrii*-infected GSB. In parallel, an additional tank with control (C; N = 50) unexposed naïve fish from the same stock was maintained with open water flow disconnected from RAS but maintaining the same temperature and oxygen conditions.

After the beginning of the exposure to *S. chrysophrii*, five samplings were performed every two weeks. In each sampling, 10 fish were euthanised by tricaine methanesulfonate (MS-222) overdose (0.1 g L^{-1}) and bled from the caudal vein using heparinised syringes. Haemoglobin (Hb) values were immediately recorded (HemoCue® Hb 201 + AB, Ängelholm, Sweden). The remaining blood was centrifuged at 3000 x *g* for 30 min, and plasma was stored at -80°C until processing. The right-sided gill arches of each R specimen were dissected to carry out *in situ S. chrysophrii* counts under a stereomicroscope to determine the infection intensity.

Ethics statement

All experiments were carried out according to the Spanish (Royal Decree RD53/2013) and the current EU (2010/63/EU) legislations on the handling of experimental fish. All procedures were approved by the Ethics and Animal Welfare Committee of the Institute of Aquaculture Torre de la Sal (IATS - CSIC, Castellón, Spain), CSIC and “Generalitat Valenciana” (permit number 2018/VSC/PEA/0240).

Plasma proteome analysis

Candidate selection

A total of 20 different plasma samples were processed for proteomic analysis by the SCSIE proteomics facility (University of Valencia, Spain), a member of the Spanish network of proteomic research facilities (Proteored). All R fish were categorised into three groups according to their infection intensity in the right-side gill arches: low, medium and high (L: 1–25; M: 26–50; H: >50 worms, respectively). Five plasma samples of each category were selected, in addition to five C samples. The remaining plasma samples were stored until use in the validation assays.

Sample preparation

For albumin depletion, 12 µl of every individual sample were precipitated with cold ethanol at a final concentration of 40% (v/v). The precipitation was incubated overnight at 5°C and then centrifuged at 15,000 x *g* for 1 hour. The albumin-containing supernatant was then removed, and the pellets air-dried. Subsequently, the pellets were dissolved in 50 µL of 0.5% sodium dodecyl sulfate in 50 mM ammonium bicarbonate. The proteins were quantified with a protein quantification assay kit (Macherey – Nagel, Germany) according to the manufacturer's instructions.

Due to the presence of lipids in the samples, 7 µg of protein were loaded in a 1D PAGE without resolving and in-gel digested. The gel slices of each sample were cut into small cubes and sequentially dehydrated with 50% acetonitrile in 50 mM ammonium bicarbonate and 100% acetonitrile. Cysteine residues were reduced by 10 mM dithiothreitol in 50 mM ammonium bicarbonate buffer at 60°C for 20 min and sulfhydryl groups were alkylated with 5.5 mM iodoacetamide in 50 mM ammonium bicarbonate in the dark at room temperature for 30 min. Gel cubes were incubated overnight at 37°C in 100 µL of 50 mM ammonium bicarbonate solution with 400 ng of trypsin. The digestions were quenched with trifluoroacetic acid (final concentration 1%). The supernatants were removed and the gel plugs were dehydrated with neat acetonitrile. The acetonitrile peptide solutions were recombined with the previous supernatants. The digestion mixture was dried in a vacuum centrifuge and resuspended in 20 µL of 2% acetonitrile, 0.1% trifluoroacetic acid.

SWATH-MS analysis

For every mixture of digested peptide, 2 µl of peptide mixture sample was loaded by an Ekspert nanoLC 425 (Eksigent, US) liquid chromatograph onto a trap column (3µ C18-CL, 350 µm x 0.5mm) and desalted with 0.1% trifluoroacetic acid at 5 µl min^{-1} during 5 min. Then, the peptides were loaded onto an analytical column (3µ C18-CL 120 Å, 75 µm x 150 mm; Eksigent) equilibrated in 5% acetonitrile 0.1% formic acid. Peptide elution was carried out with a linear gradient of 7–40% acetonitrile with 0.1% formic acid at a flow rate of 300 nL min^{-1}. Peptides were analysed in a nanoESI qQTOF mass spectrometer (6600plus TripleTOF, ABSCIEX). The samples were ionised in a Source Type: Optiflow < 1 µL Nano applying 3.0 kV to the spray emitter at 200°C. The TripleTOF was operated in swath mode, in which a 0.050-s TOF-MS scan from 350–1250 m z^{-1} was performed. After, 0.080 s product ion scans were acquired in 100 variable windows from 400 to 1250 m z^{-1}. The total cycle time was 2.79 sec. The individual SWATH injections were randomised to avoid bias in the analysis. Previously, a pooled sample was injected to determine the best gradient and sample amount.

Spectral library building

Plasma aliquots of all the samples were pooled to build the spectral library by in-gel digestion and LC-MS/MS with data-dependent acquisition (DDA) in order to separate and identify the proteins present in the samples. After resolving the 1D-SDS-PAGE, the gel career corresponding to the library was cut into pieces, each of which was digested with trypsin, extracted with acetonitrile, dried and resuspended as described above. Exactly as described before, each library sample was first loaded into a trap column and then into an analytical column, before loading the eluted peptides in the nanoESI qTOF mass

spectrometer for analysis in DDA mode. Survey MS1 scans were acquired from 350–1400 m/z for 250 ms. The quadrupole resolution was set to 'LOW' for MS2 experiments, which were acquired 100–1500 m/z for 25 ms in 'high sensitivity' mode. The following switch criteria were used: charge: 2 + to 4+; minimum intensity; 100 counts per second (cps). Up to 100 ions were selected for fragmentation after each survey scan. Dynamic exclusion was set to 15 s.

The obtained DDA data files were processed by means of the ProteinPilot v5.0 (ABSciex) search engine and a single list of peaks was generated using the default parameters and combining the acquired information of all gel fragments. The Paragon algorithm (ProteinPilot) was used to search against 279,921 sequences available in GSB protein databases (NCBI, UniProt and transcriptome from the genome assembly [30]. A false discovery rate (FDR) correction was applied for the validation of the data. The identified proteins were grouped based on MS/MS spectra by the ProteinPilot Pro Group Algorithm to avoid using the same spectral evidence for more than one protein. The protein within each group that could explain more spectral data with a 95% confidence threshold was depicted as the primary protein of the group. To increase the spectral data with DIA information the data from the pooled samples were analysed by DIA Umpire as previously published [31].

Protein quantification

The SCIEX.wiff data-files obtained from SWATH runs of individual plasma samples, were loaded into PeakView v2.1 (SCIEX) with the generated spectral library consisting of a combination of data-dependent and independent acquisition information, obtained from the pooled sample interrogated in the available protein databases at a peptide confidence threshold of 95% confidence and an FDR < 1. The extracted ion chromatograms were integrated, and peak areas were used to calculate the total protein quantity.

Validation assays

In order to corroborate some of the findings of the proteomic analysis, three assays were performed in plasma samples from all sampled fish, including the ones used in the proteomics study.

Plasma complement assay

The lytic activity of the alternative complement pathway (ACP) was determined using sheep red blood cells (SRBC) as targets, and the dilution corresponding to 50% haemolysis ml^{-1} was expressed as ACH50. This assay was performed following the procedure described in [32], using 2.85×10^8 SRBC ml^{-1}.

Plasma cholesterol assay

Plasma cholesterol was measured using the Infinity Cholesterol Liquid Stable Reagent (ThermoFisher Scientific, Waltham, MA, USA) following the manufacturer's instructions. A calibration curve was performed using serial dilutions of Cholesterol (Sigma, St. Louis, MO, USA). The amount of plasma per reaction was 4 µl. Reactions were performed in duplicate.

Plasma biotin detection

Plasma biotin was measured using the Biotin Quantitation Kit (Abcam, Cambridge, UK) following the manufacturer's instructions using 30 µl of plasma in duplicate. Biotinylated BSA was used as a positive control. A standard curve was prepared using biotin concentrations ranging between 20 and 1000 µM.

Data and statistical analysis

The protein areas obtained with PeakView® v2.1 software (SCIEX, US) were normalised by the total sum of the areas of all the quantified proteins. Normalised data were used to build a partial least squares-discriminant analysis (PLS-DA) model using the Bioconductor R package *ropls* [33]. The PLS-DA model quality was evaluated with the fit (R2Y(cum)) and prediction (Q2 (cum)) indicators. A validation test consisting of 500 random permutations was performed to discard overfitting of the PLS-DA model. The contribution of the different proteins to the group separation was determined by variable importance in projection (VIP) values. A VIP value > 1 was considered the threshold to determine discriminant proteins in the PLS-DA model [34–36]. Hierarchical clustering, heatmap representation and k-means analyses were performed with the normalised area values of all discriminant proteins (VIP > 1) using iDEP.95 [37].

To perform a pathway analysis, the discriminant protein identifiers were converted to their human equivalents, when possible, and analysed with the Bioconductor *ReactomePA* R package [38].

The R package *corrplot* was used to calculate correlations between the different proteins and the infection intensity applying the *cor.test* function to compute significant correlation coefficients with a confidence level of 0.95.

All data were checked for normality prior to any statistical analysis. Statistical differences between C and R (L, M, H) haemoglobin, ACP, cholesterol and biotin values were calculated using a one-way ANOVA and a post hoc multiple comparisons Holm-Šídák test. Differences were considered significant at $p < 0.05$ and a power analysis was performed in every test. All statistical analyses were performed using SigmaPlot v.14.0 (Systat Software, Inc., San Jose California USA).

Results

Plasma proteome analysis

A total of 291 gilthead sea bream proteins were identified and quantified in the plasma samples. The normalised abundance values of each sample were used to construct a PLS-DA model to determine differences amongst groups. The PLS-DA model was based on five components (Additional file 1A) which explained 98.8% (R2Y) and predicted 70% (Q2Y) of the total variance (Fig. 1A). No outliers were detected during this analysis (Additional file 1C), and the model was validated using a permutation test (Additional file 1B). The PLS-DA model clearly separated the C group from the R fish. The dispersion of the C samples in the plot showed great individual variability in this group (Fig. 1A). Highly infected fish (H) formed a separated group, whereas medium and low infected fish (M/L) were not significantly

separated by the model, constituting a single set. Recipient fish (H and M/L groups) showed lower variability in their proteomic profiles than the C group.

The PLS-DA model yielded 129 proteins with VIP values > 1 (Additional file 2). These differentially abundant proteins driving the separation of the different groups were further explored in a heatmap. Hierarchical clustering showed again a clear separation in three groups: C, M/L and H, validating the results obtained from the PLS-DA (Fig. 1B). K-means analysis, conducted to visualise expression patterns among the differentially abundant proteins, revealed four clear clusters (Fig. 2). Cluster A consisted of 20 proteins that were more abundant in the C samples than in R samples. Cluster B grouped 46 proteins more abundant in the highly infected samples (H) than in the other two groups. Cluster C contained 41 proteins with high abundance in the M/L group, low abundance in the H group, and intermediate values in the C group. Cluster D comprised 22 proteins with low presence in C samples and increased in R fish.

Pathway analysis

In an attempt to clarify the biological significance of the changes observed in the plasma proteome of the different groups, pathway analysis was performed with the differentially abundant proteins classified in the four k-means clusters. Enriched pathways in R GSB were coherent with functions expected to be found in plasma, highlighting an enrichment in pathways related to haemostasis, immune system, metabolism of vitamins and proteins, and transport of lipoproteins or O_2/CO_2 (Fig. 3). Among the pathways associated with the immune system, the complement system was highly represented. Overall, the most represented function was related to lipid (cholesterol) transport.

Proteins correlated with infection intensity

Correlation analysis revealed that 22 proteins significantly correlated with the infection degree (Table 1). Fourteen proteins, including three apolipoproteins, two globins, complement C3, ceruloplasmin, and biotinidase, were negatively correlated with the infection intensity. Conversely, 8 proteins exhibited a positive correlation with the disease.

Table 1

Plasma proteins whose abundances significantly correlated with Sparicotyle chrysophrii **infection degree**. Negative and positive correlations and the strength of each correlation are shown by the sign and value of the correlation coefficient (Corr. Coef.). Significant correlations were assumed when *p.* val < 0.05.

Protein	Corr. Coef.	*p.* val
Saxitoxin and tetrodotoxin-binding protein 1-like	-0.65	0.002
Alpha-2 globin	-0.62	0.003
Immunoglobulin light chain, partial	-0.61	0.005
Biotinidase	-0.58	0.007
Apolipoprotein B-100	-0.56	0.010
Ectonucleotide pyrophosphatase/phosphodiesterase family member 2	-0.54	0.014
Complement C3-like	-0.51	0.020
Apolipoprotein H	-0.50	0.024
Carboxypeptidase N subunit 2	-0.49	0.030
Beta globin	-0.48	0.033
Apolipoprotein A-II	-0.48	0.033
Ceruloplasmin	-0.47	0.037
Serpin family G member 1	-0.45	0.048
Ladderlectin-like	-0.45	0.048
Immunoglobulin lambda chain C region	0.57	0.009
Hibernation-specific plasma protein HP-55	0.56	0.010
L-rhamnose-binding lectin CSL2	0.53	0.016
Alpha-1-microglobulin	0.52	0.018
Cyclin dependent kinase like 1	0.47	0.036
Serotransferrin	0.46	0.039
Coagulation factor X-like	0.46	0.040
Estrogen-regulated protein	0.45	0.048

Validation assays

Haemoglobin values (Fig. 4), plasma cholesterol concentrations (Fig. 5) and ACP (Fig. 6) showed a gradual and significant decrease with infection intensity. These results validated the detected gradual decline of plasma alpha-2 and beta globins, apolipoproteins B-100, H and A-II, and complement C3 at the

protein level. On the other hand, no significant differences were detected in plasma biotin levels, and the measured values were very close to the lower detection threshold of the technique (Additional file 3).

Discussion

Fish gills are responsible for several vital physiological functions other than respiration, such as osmoregulation, excretion of nitrogenous waste, pH regulation, hormone production [39] and homeostatic regulation of copper [40]. Compromised gill function would inevitably alter these physiological functions, hence the importance of assuring gill health. Despite the impact on animal welfare and the economic repercussions, little is known about the effect of *S. chrysophrii* in GSB. The plasma proteomic profile from healthy and *S. chrysophrii*-infected GSB was assessed via a SWATH-MS analysis to better understand the host-parasite interactions and broaden the knowledge of the pathogenesis of sparicotylosis.

The discriminant analysis of the abundance of all detected proteins formed three different groups (C, M/L and H). The dispersal among the healthy GSB (C) group was clearly greater than among diseased fish (M/L and H groups) (Fig. 1A). However, differentially abundant proteins in the M/L group showed a greater disparity than in the H group, which in turn seemed closer to the C group phenotype in both the PLS-DA model and heatmap (Fig. 1). These observations suggest that the hosts suffer a profound imbalance when suffering mild (M/L) *S. chrysophrii*-infection intensities, as observed by Piazzon et al. 2019 [19]. In GSB surviving to high parasitic burdens (H), the detected proteomic profile seems to indicate an onset of compensation mechanisms to restore homeostasis, getting closer to the profile of C fish. In sparicotylosis, such homeostasis recovery might be the result of the monogeneans' intimate coevolution with their hosts [41, 42]. Under farming conditions, with high stocking densities, exposure to environmental stressors, high infection pressures and recurrent sparicotylosis infections once the disease is established, high mortality is reported, even after receiving treatment. Apparently, under these harsh farming conditions, fish would be unable to recover homeostasis, resulting the pathogenic effect of the parasite more devastating. Hence, future proteomic plasma studies of moribund GSB from sea cages suffering sparicotylosis would shed some light on this issue. However, the current results were obtained in a time-limited exposure (10 weeks) and under a relatively bounded parasite multiplication context compared to an enzootic farm. Under these conditions, the observed attempt of homeostatic restitution in highly infected fish raises the question of whether an earlier stimulation of these mechanisms by some dietary or health interventions would be feasible, in order to mitigate the effects of the disease.

Sparicotyle chrysophrii modulated proteins involved in several biological processes in GSB. Among them, the levels of various proteins increased and decreased in a complex network of interactions. The main pathways severely modulated by *S. chrysophrii* were those related to haemostasis, lipid metabolism and transport, and the immune system (Fig. 3).

Haemostasis

Polyopisthocotylean monogeneans have been described as hematophagous parasites [43, 44], but it has not been until recently that the haematophagous nature of *S. chrysophrii* has been demonstrated experimentally [45]. From the current study, we can discern a clear negative impact on the GSB's haemostasis. Blood haemoglobin significantly dropped as the parasite burden increased (Fig. 4). These low Hb values mirrored the plasma proteomic results, where the main Hb constituents, alpha-2 and beta globins, negatively and significantly correlated with the infection intensity (Table 1, Fig. 4). In addition, alpha-1-microglobulin, a radical scavenger dealing with heme toxicity and erythroprotective anti-haemolytic effects in humans [46], presented a positive and significant correlation (Table 1). This suggests that *S. chrysophrii*-infected GSB suffer from haemolytic anaemia, as occurs in hosts facing a haemolytic insult, which leads to the release of Hb and free heme groups from erythrocytes, increasing the oxidative stress [46]. Overall, these results would imply anaemia and oxygen transport impairment, explaining hypoxia and lethargy signs observed in parasitised fish.

The coagulation cascade also seems to be triggered by sparicotylosis. In mammalian [47, 48] and fish [49] blood, the extrinsic pathway is initiated following tissue damage and subsequent exposure of subendothelial tissue factor (TF) to Factor VII, whereas the intrinsic pathway is triggered by the exposure of a foreign negatively charged surface to Factor XII. Both pathways converge in Factor X, after which the common pathway of the coagulation cascade follows, resulting in the production of thrombin and leading to clot formation and final restoration of haemostasis [47, 48]. In the current study, most proteins involved in the coagulation cascade were represented in cluster B of the K-means analysis (Fig. 2). In GSB suffering sparicotylosis, both intrinsic (Factor IX) and extrinsic (Factor VII) pathways of the coagulation cascade as well as common pathway of the coagulation cascade (Factor X and Factor V) were modulated (Additional file 2). It is noteworthy that, unlike in the M/L group, all coagulation factors in cluster B were upregulated in the H group (Fig. 2), in agreement with the significantly positive correlation of Factor X with the infection intensity (Table 1). Thus, the coagulation capacity of GSB apparently increased when high parasitic burdens were reached. Similarly, in several tick species, different proteins with anticoagulant properties affecting the intrinsic, extrinsic and common coagulation pathways [50–52] have been described and characterised, suggesting that these haematophagous parasites can modulate their host's haemostasis at different levels.

Since *S. chrysophrii* is an ectoparasite and not an intravascular parasite, we suspect that the intrinsic pathway could be, in part, triggered by RBCs fragment remnants [53] resulting from haemolysis. In contrast, the activation of the extrinsic pathway, may be due to tissue disruption induced by the parasite's feeding mechanisms and its haptor.

Lipid metabolism and transport

Different parasitic species, ranging from Protozoa to Metazoa, have been described to alter the lipidic profile of their host species in fish [54] as well as in higher vertebrates [55–64]. In particular, Platyhelminthes are unable to synthesise fatty acids *de novo* [65]; thus, they rely on the host's lipid reservoir to ensure their survival. Several fatty acid binding proteins (FABPs) have been identified in trematode species such as *Schistosoma* spp., *Fasciola* spp, and most recently in the diplozoid

monogenean *Eudiplozoon nipponicum* [66, 67]. Even though FABPs have been described to play a role in fatty acid uptake in *F. hepatica* from host blood and in immunomodulation, their function in monogeneans remains unknown [66]. Our results show that apolipoprotein B-100 (ApoB-100) and apolipoprotein A-II (ApoA-II) were negatively and significantly correlated with the infection intensity (Table 1; Fig. 5). In addition, cholesterolaemia values in plasma samples of *S. chrysophrii* - infected GSB were significantly lower than in the C group, supporting our proteomic results (Fig. 5). Reduction of plasma cholesterol in GSB was also triggered by environmental stressors [68, 69]) and dietary intervention involving the replacement of fish meal and oil by vegetable ingredients [32, 70]. The latter provoked a simultaneous drop in plasma cholesterol and blood Hb, which was reversed by a butyrate additive in the diet. This finding could open a path for the use of butyrate as a mitigation strategy for the effects of sparicotylosis.

ApoB-100 is a crucial structural component in very-low-density lipoproteins (VLDL) and low-density lipoproteins (LDL), predominantly composed of triglycerides and cholesteryl esters, respectively. ApoA-II, on the other hand, is associated with high-density lipoproteins (HDL_2 and HDL_3), predominantly composed of cholesteryl esters [71, 72]. Our results suggest a dependency of *S. chrysophrii* on its host's lipid reservoir. However, the mechanisms by which *S. chrysophrii* would rely on the host's lipids remain unknown.

Plasma lipoproteins (LDLs and HDLs) play an essential role in host defence as a component of the immune system [73–75] and against bacterial, viral and parasitological infections [73] in mammals. Hence, in our fish-parasite model, an alteration in lipoprotein levels could render the host more susceptible to secondary infections. Moreover, other roles in haemostasis have been granted to LDLs and HDLs, thus somewhat contributing to the control of haematological parameters, such as RBC membrane stability [76].

Immune system

Differences regarding the host's immune response have been observed between monopistholocotylean and polyopisthocotylean monogenean parasites [77]. These differences have been suggested to lie in the different feeding strategies [77], since polyopisthocotylean monogeneans are generally considered haematophagous. Hence, they need to evade the host's immune response to ensure their feeding and survival. Our study shows how *S. chrysophrii* infection changes the abundance of several complement proteins (factor H, factor B, factor I, C1q, C3, C4, C5, C6, C7, C8; Additional file 2), inducing an inhibition of the alternative pathway as the infection intensity increases (Fig. 6). In the same line, other studies with the same host and parasite species revealed that this parasite downregulated *c3* splenic expression [19] and lowered complement levels in serum [18]. A local downregulation of *c3* expression has also been described in other monogenean infections [78, 79]. The depletion of complement effectors in GSB plasma worsened during the infection, compromising the fish immunocompetence. Further in-depth studies regarding the host's immune response during monogenean parasite infections and, in particular, polyopisthocotylean monogeneans are required to fully understand the exact mechanisms involved. Our results point to a complex network regulating the innate immune response, including SERPINs and

ceruloplasmin, which may indirectly modulate the complement system, resulting in neutrophil activation and inflammation.

Proteins linking haemostasis and immune system

Serine-protease inhibitors (SERPINs)

Serine proteases are conserved enzymes throughout evolution that have a crucial role in several physiological processes, including blood coagulation, fibrinolysis, inflammation and immune response. SERPINs obtain their name from serine protease inhibitors. Still, they are a superfamily of proteins that primarily regulate the proteolytic pathways of serine and cysteine proteases [80–83].

It has been described that protease inhibitors may have a leading role in host-parasite interactions and, more specifically, in evasion mechanisms and survival on the parasite's behalf [84–86]. Interestingly, two protease inhibitors similar to SERPING1 in terms of function, EnSerp1 and EnKT1, have been characterised in the monogenean *Eudiplozoon nipponicum* [87, 88].

Some authors suggested that some digenean trematode parasites could have the ability to modulate the host's SERPINs [25]. In several parasitic species, including ticks [50, 51, 89], copepods [90], digenean [91–94], and monogenean [66, 87, 88, 95–98] trematodes, endogenous proteases and protease inhibitors potentially acting as virulence factors have been described and characterised.

In the current study, three SERPINs were differentially expressed upon infection; SERPINA1 (α_1–antitrypsin), SERPIND1 (heparin coagulation factor II) and SERPING1 (C1-inhibitor; C1INH) (Additional file 2). SERPINA1 was grouped in cluster C (more abundant in M/L group), whereas both SERPIND1 and SERPING1 were grouped in cluster B (more abundant in H) (Fig. 2).

SERPINA1 inhibits neutrophil elastase, a serine protease with microbiocidal effects involved in the acute phase of the inflammation process and tissue remodelling [99]. We relate this observation to an early impairment of an inflammatory response elicited by neutrophils. This event could be driven by a deliberate modulation of SERPINA1 by *S. chrysophrii* as an evasion mechanism, in order to enable attachment to gill filaments. Similar effects on SERPINA1 have been observed in murine *Toxoplasma gondii* infections [26], but no records are available on SERPINA1 being modulated by fish parasites.

Both SERPIND1 and SERPING1 have a key role in coagulation; however, SERPING1 also affects the immune system. SERPIND1 is known to, directly and indirectly, inhibit thrombin in the common pathway of the coagulation cascade [80, 81, 100], thus preventing the fibrinogen and platelet activation and ultimately preventing the clot formation and haemostasis restoration. At a haemostatic level, SERPING1 inhibits several components within the intrinsic coagulation pathway (plasma kallikrein, activated Factor XII (FXIIa) and XI (FXIa)) as well as fibrinolytic proteases (plasmin, tPA and uPA). Further SERPING1 inhibitory abilities extend to both C1s and C1r, proteases responsible for the activation and proteolytic activity of the C1 complex of the classic complement pathway [47, 48, 80, 81, 83, 101–103].

Thus, the significantly higher abundance of SERNPIND1 and SERPING1 in GSB with high parasitic burdens could imply an anticoagulant and innate immunosuppressor effect in these hosts (Fig. 2). However, within cluster B, SERPING1 shows a significant negative correlation with the infection intensity (Table 1). SERPINs operate within a complex physiological modulation network, and further SERPIN-targeted studies are needed to unravel this paradox, as well as the opposing coagulant and anticoagulant actions of serpins and the coagulation cascade. Counter-regulation evidenced by our results might be the effect of the host response aiming for homeostatic balance or a host *vs* parasite modulation.

Ceruloplasmin

Ceruloplasmin is an acute-phase protein that has been associated with inflammation, severe infection and tissue damage in mammals and fish. Ceruloplasmin has also been described as a copper-carrying protein, ultimately having a role in hypoxic vasodilation and ischemia-reperfusion cytoprotection [104–106], and having the ability to oxidise toxic plasma ferrous iron into its ferric form to be transported by transferrin [105]. Moreover, under hyperammonaemia conditions, the intrinsic pathway of the coagulation cascade is triggered, and the functional activity of platelets decreases. However, ceruloplasmin can prevent haemostatic disorders by restoring platelet functionality and preventing hypercoagulation [107].

Henry et al. 2015 previously described no significant differences in ceruloplasmin activity in GSB after a 10 week-long *S. chrysophrii* infection. Our results suggest an initial increase in plasma ceruloplasmin levels in M/L followed by a later decrease during the course of infection in H group. Thus, we hypothesize that fish with lower infection intensities were in an acute phase of the disease, while H GSB restored their ceruloplasmin to control levels in agreement with the observations of Henry et al. 2015.

Conclusions

Understanding how GSB responds to *S. chrysophrii* is critical for developing new treatments and health-management strategies in the aquaculture industry. The present plasma proteomic study of *S. chrysophrii*-infected GSB gives a crucial global overview of the pathogenesis of sparicotylosis, representing a valuable contribution to the understanding of the disease and highlighting new targets for further research. Sparicotylosis profoundly alters the haemostasis, the innate immune system and the lipid metabolism and transport in GSB. However, in high intensity experimental infections, GSB seems to attempt to restore some of the alterations suffered during the acute phase of the disease. This could be either due to the close evolutionary ties between *S. chrysophrii* and GSB, or to a host protection mechanism against the damage caused by the activation of acute mechanisms.

List Of Abbreviations

GSB, gilthead sea bream; C, control; R, recipient; L. low; M, medium; H, high

Declarations

Ethics approval and consent to participate

An ethics statement on the use of experimental animals is included in the Methods section.

Consent for publication

Not applicable.

Availability of data and materials

The proteomics data has been deposited in the PRIDE repository, with the dataset identifier PXD034541. The rest of the data generated by this study is included in the manuscript and in the additional files.

Competing interests

The authors declare no competing interests.

Funding

This work has been financed by the Spanish Ministry of Science and Innovation and Universities project (SpariControl, RTI2018-098664-B-I00, AEI/FEDER, UE). ERF was supported by an FPI contract PRE2019-087409. MCP was funded by a Ramón y Cajal Postdoctoral Research Fellowship (RYC2018-024049-I & ACOND/2022 Generalitat Valenciana). RDP was contracted under the PTA Programme from the Spanish Ministry of Science, Innovation and Universities (PTA2018-015315-I). Both MCP and RDP contracts were co-funded by the European Social Fund (ESF).

Authors contributions

ERF, Methodology, Investigation, Formal analysis, Writing original draft; MCP, Investigation, Formal analysis, Data curation, Visualization; RDP, Investigation, Writing original draft; OP, Supervision, Funding acquisition; IE, Methodology, Formal analysis, Investigation, Data curation, Visualization, Supervision, Writing original draft; ASB, Methodology, Supervision, Project administration, Funding acquisition. All authors read and approved the final manuscript.

Acknowledgements

The authors thank Prof. J. Pérez-Sánchez from the Nutrigenomics and Fish Growth Endocrinology group (IATS, CSIC) for providing access to genomic database of GSB, M. Luz Valero from SCSIE proteomics facility (University of Valencia, Spain) for the proteomics analyses and support, and I. Vicente for technical assistance with fish husbandry and samplings at IATS.

References

1. Repullés-Albelda A, Raga JA, Montero FE. Post-larval development of the microcotylid monogenean *Sparicotyle chrysophrii* (Van Beneden and Hesse, 1863): Comparison with species of Microcotylidae and Heteraxinidae. Parasitol Int. 2011;60:512–20.
2. Repullés-Albelda A, Holzer AS, Raga JA, Montero FE. Oncomiracidial development, survival and swimming behaviour of the monogenean *Sparicotyle chrysophrii* (Van Beneden and Hesse, 1863). Aquaculture. 2012;338–341:47–55.
3. Mladineo I. Parasite communities of Adriatic cage-reared fish. Dis Aquat Organ. 2005;64:77–83.
4. Sánchez-García N, Raga JA, Montero FE. Veterinary Parasitology Risk assessment for parasites in cultures of *Diplodus puntazzo* (Sparidae) in the Western Mediterranean: Prospects of cross infection with *Sparus aurata*. Vet Parasitol. 2014;204:120–33.
5. Mladineo I, Maršić-Lučić J. Host Switch of *Lamellodiscus elegans* (Monogenea: Monopisthocotylea) and *Sparicotyle chrysophrii* (Monogenea: Polyopisthocotylea) between Cage-reared Sparids. Vet Res Commun. 2007;31:153–60.
6. Mladineo I, Šegvić T, Grubišić L. Molecular evidence for the lack of transmission of the monogenean *Sparicotyle chrysophrii* (Monogenea, Polyopisthocotylea) and isopod *Ceratothoa oestroides* (Crustacea, Cymothoidae) between wild bogue (*Boops boops*) and cage-reared sea bream (*Sparus aurata*) and sea bass (*Dicentrarchus labrax*). Aquaculture. 2009;295:160–7.
7. Katharios P, Papandroulakis N, Divanach P. Treatment of Microcotyle sp. (Monogenea) on the gills of cage-cultured red porgy, *Pagrus pagrus* following baths with formalin and mebendazole. Aquac Eng. 2006;251:167–71.
8. FEAP. European Aquaculture Production Report [Internet]. FEAP Prod. Rep. – 2020. 2020. Available from: https://feap.info/wp-content/uploads/2020/10/20201007_feap-production-report-2020.pdf
9. Sitjà-Bobadilla A, de Felipe MC, Álvarez-Pellitero P. *In vivo* and *in vitro* treatments against *Sparicotyle chrysophrii* (Monogenea: Microcotylidae) parasitizing the gills of gilthead sea bream (*Sparus aurata* L.). Aquaculture. 2006;261:856–64.
10. Sitjà-Bobadilla A, Alvarez-Pellitero P. Experimental transmission of *Sparicotyle chrysophrii* (Monogenea: Polyopisthocotylea) to gilthead seabream (*Sparus aurata*) and histopathology of the infection. Folia Parasitol (Praha). 2009;56:143–51.
11. Fioravanti ML, Mladineo I, Palenzuela O, Beraldo P, Massimo M, Gustinelli A, et al. Fish farmer's guide to combating parasitic infections in european sea bass and gilthead sea bream aquaculture [Internet]. ParaFishControl. 2020. Available from: https://www.parafishcontrol.eu/parafishcontrol-results/parafishcontrol-deliverables
12. Mladineo I, Trumbić Ž, Ormad-García A, Palenzuela O, Sitjà-Bobadilla A, Manuguerra S, et al. *In vitro* testing of alternative synthetic and natural antiparasitic compounds against the monogenean *Sparicotyle chrysophrii*. Pathogens. 2021;10.
13. Merella P, Montero FE, Burreddu C, Garippa G. In-feed trials of fenbendazole and other chemical/natural compounds against *Sparicotyle chrysophrii* (Monogenea) infections in Sparus aurata (Osteichthyes). Aquac Res. 2021;52:5908–11.

14. Bögner D, Bögner M, Schmachtl F, Bill N, Halfer J, Slater MJ. Hydrogen peroxide oxygenation and disinfection capacity in recirculating aquaculture systems. Aquac Eng. 2021;92.
15. European Chemicals Agency - ECHA. Formaldehyde and formaldehyde releasers - Strategy for future work [Internet]. 2018. Available from: https://echa.europa.eu/documents/10162/17233/formaldehyde_review_report_en.pdf/551df4a2-28c4-2fa9-98ec-c8d53e2bf0fc?t=1516270136797
16. European Chemicals Agency - ECHA. Substance Evaluation Conclusion as require by REACH Article 48 and Evaluation Report for Formaldehyde [Internet]. 2019. Available from: https://echa.europa.eu/documents/10162/cc0acabf-6e82-f2ed-5dbe-8058f48ce6c4
17. Leal JF, Neves MGPMS, Santos EBH, Esteves VI. Use of formalin in intensive aquaculture: properties, application and effects on fish and water quality. Rev Aquac. 2018;10:281–95.
18. Henry MA, Nikoloudaki C, Tsigenopoulos C, Rigos G. Strong effect of long-term *Sparicotyle chrysophrii* infection on the cellular and innate immune responses of gilthead sea bream, *Sparus aurata*. Dev Comp Immunol. 2015;51:185–93.
19. Piazzon MC, Mladineo I, Naya-Català F, Dirks RP, Jong-Raadsen S, Vrbatović A, et al. Acting locally - Affecting globally: RNA sequencing of gilthead sea bream with a mild *Sparicotyle chrysophrii* infection reveals effects on apoptosis, immune and hypoxia related genes. BMC Genomics. 2019;20:1–16.
20. Liu RD, Cui J, Liu XL, Jiang P, Sun GG, Zhang X, et al. Comparative proteomic analysis of surface proteins of *Trichinella spiralis* muscle larvae and intestinal infective larvae. Acta Trop. 2015;150:79–86.
21. Suttiprapa S, Sotillo J, Smout M, Suyapoh W, Chaiyadet S, Tripathi T. *Opisthorchis viverrini* proteome and host e parasite interactions. Adv Parasitol. 2018;102:45–72.
22. Cui S, Xu L, Zhang T, Xu M, Yao J, Fang C, et al. Proteomic characterization of larval and adult developmental stages in *Echinococcus granulosus* reveals novel insight into host – parasite interactions. J Proteomics. 2013;84:158–75.
23. Tu V, Mayoral J, Sugi T, Tomita T, Han B, Weiss LM. Enrichment and proteomic characterization of the cyst wall from *in vitro Toxoplasma gondii* cysts. MBio. 2019;10:1–15.
24. Marzano V, Pane S, Foglietta G, Mortera SL, Vernocchi P, Muda AO, et al. Mass spectrometry based-proteomic analysis of *Anisakis* spp.: A preliminary study towards a new diagnostic tool. Genes (Basel). 2020;11:1–18.
25. Zhang FK, Hu RS, Elsheikha HM, Sheng ZA, Zhang WY, Zheng W Bin, et al. Global serum proteomic changes in water buffaloes infected with *Fasciola gigantica*. Parasites and Vectors. 2019;12.
26. Zhou C, Xie S, Li M, Huang C, Zhou H, Cong H. Analysis of the serum peptidome associated with *Toxoplasma gondii* infection. J Proteomics. 2020;222:1–9.
27. Gillis-Germitsch N, Kockmann T, Kapel CMO, Thamsborg SM, Webster P, Tritten L, et al. Fox serum proteomics analysis suggests host-specific responses to *Angiostrongylus vasorum* infection in canids. Pathogens. 2021;10:1–16.

28. Raza A, Schulz BL, Nouwens A, Jackson LA, Piper EK, James P, et al. Serum proteomes of Santa Gertrudis cattle before and after infestation with *Rhipicephalus australis* ticks. Parasite Immunol. 2021;43:1–13.
29. Kuleš J, Lovrić L, Gelemanović A, Ljubić BB, Rubić I, Bujanić M, et al. Complementary liver and serum protein profile in wild boars infected by the giant liver fluke *Fascioloides magna* using tandem mass tags quantitative approach. J Proteomics. 2021;247.
30. Pérez-Sánchez J, Naya-Català F, Soriano B, Piazzon MC, Hafez A, Gabaldón T, et al. Genome sequencing and transcriptome analysis reveal recent species-specific gene duplications in the plastic gilthead sea bream (*Sparus aurata*). Front Mar Sci. 2019;6:1–18.
31. Tsou CC, Avtonomov D, Larsen B, Tucholska M, Choi H, Gingras AC, et al. DIA-Umpire: Comprehensive computational framework for data-independent acquisition proteomics. Nat Methods. 2015;12:258–64.
32. Sitjà-Bobadilla A, Peña-Llopis S, Gómez-Requeni P, Médale F, Kaushik S, Pérez-Sánchez J. Effect of fish meal replacement by plant protein sources on non-specific defence mechanisms and oxidative stress in gilthead sea bream (*Sparus aurata*). Aquaculture. 2005;249:387–400.
33. Thévenot EA, Roux A, Xu Y, Ezan E, Junot C. Analysis of the human adult urinary metabolome variations with age, body mass index, and gender by implementing a comprehensive workflow for univariate and OPLS statistical analyses. J Proteome Res. 2015;14:3322–35.
34. Wold S, Sjöström M, Eriksson L. PLS-regression: A basic tool of chemometrics. Chemom Intell Lab Syst. 2001;58:109–30.
35. Kieffer DA, Piccolo BD, Vaziri ND, Liu S, Lau WL, Khazaeli M, et al. Resistant starch alters gut microbiome and metabolomic profiles concurrent with amelioration of chronic kidney disease in rats. Am J Physiol - Ren Physiol. 2016;310:F857–71.
36. Li H, Ma ML, Luo S, Zhang RM, Han P, Hu W. Metabolic responses to ethanol in *Saccharomyces cerevisiae* using a gas chromatography tandem mass spectrometry-based metabolomics approach. Int J Biochem Cell Biol. Elsevier Ltd; 2012;44:1087–96.
37. Ge SX, Son EW, Yao R. iDEP: An integrated web application for differential expression and pathway analysis of RNA-Seq data. BMC Bioinformatics. BMC Bioinformatics; 2018;19:1–24.
38. Yu G, He QY. ReactomePA: An R/Bioconductor package for reactome pathway analysis and visualization. Mol Biosyst. Royal Society of Chemistry; 2016;12:477–9.
39. Farrell AP. Volume 2: Gas exchange, internal homeostatis, and food uptake. Encycl. Fish Physiol. From Genome to Environ. 2011.
40. Wang X, Wang WX. Homeostatic regulation of copper in a marine fish simulated by a physiologically based pharmacokinetic model. Environ Pollut. 2016;218:1245–54.
41. Kearn GC. Evolutionary expansion of the Monogenea. Int J Parasitol. 1994;24:1227–71.
42. Poulin R. The evolution of monogenean diversity. Int J Parasitol. 2002;32:245–54.

43. Llewellyn J. Observations on the food and the gut pigment of the polyopisthocotylea (Trematoda: Monogenea). Parasitology. 1954;44:428–37.
44. Halton DW, Jennings JB. Observations on the nutrition of monogenetic trematodes. Biol Bull. 1965;129:257–72.
45. Riera-Ferrer E, Estensoro I, Piazzon C, Del Pozo R, Palenzuela O, Sitjà-Bobadilla A. Unveiling the blood-feeding behaviour of the gill parasite *Sparicotyle chrysophrii*. EAFP 20th Int Conf Dis Fish Shellfish. 2021. p. 35.
46. Kristiansson A, Gram M, Flygare J, Hansson SR, Åkerström B, Storry JR. The role of α1-microglobulin (a1m) in erythropoiesis and erythrocyte homeostasis — therapeutic opportunities in hemolytic conditions. Int J Mol Sci. 2020;21:1–22.
47. Smith SA, Travers RJ, Morrissey JH. How it all starts: initiation of the clotting cascade. Crit Rev Biochem Mol Biol. 2015;50:326–36.
48. He S, Cao H, Thålin C, Svensson J, Blombäck M, Wallén H. The clotting trigger is an important determinant for the coagulation pathway *in vivo* or *in vitro*-inference from data review. Semin Thromb Hemost. 2021;47:63–73.
49. Tavares-Dias M, Oliveira SR. A review of the blood coagulation system of fish. Brazilian J Biosci. 2009;7:205–24.
50. Parizi LF, Ali A, Tirloni L, Oldiges DP, Sabadin GA, Coutinho ML, et al. Peptidase inhibitors in tick physiology. Med Vet Entomol. 2018;32:129–44.
51. Kotál J, Polderdijk SGI, Langhansová H, Ederová M, Martins LA, Beránková Z, et al. *Ixodes ricinus* salivary serpin iripin-8 inhibits the intrinsic pathway of coagulation and complement. Int J Mol Sci. 2021;22.
52. Ehebauer MT, Mans BJ, Gaspar ARM, Neitz AWH. Identification of extrinsic blood coagulation pathway inhibitors from the tick *Ornithodoros savignyi* (Acari: Argasidae). Exp Parasitol. 2002;101:138–48.
53. Cappellini MD. Coagulation in the Pathophysiology of Hemolytic Anemias. Am Soc Hematol. 2007;74–8.
54. Yuskiv LL, Yuskiv ID. The lipid metabolism in carp during invasion by the tapeworm *Bothriocephalus acheilognathi*. Regul Mech Biosyst. 2020;11:214–9.
55. Luján HD, Mowatr MR, Byrd LG, Nash TE. Cholesterol starvation induces differentiation of the intestinal parasite *Giardia lamblia*. Proc Natl Acad Sci USA. 1996;93:7628–33.
56. Coppens I, Sinai AP, Joiner KA. *Toxoplasma gondii* exploits host low-density lipoprotein receptor-mediated endocytosis for cholesterol acquisition. J Cell Biol. 2000;149:167–80.
57. Sonda S, Ting LM, Novak S, Kim K, Maher JJ, Farese R V., et al. Cholesterol Esterification by Host and Parasite Is Essential for Optimal Proliferation of *Toxoplasma gondii*. J Biol Chem. 2001;276:34434–40.

58. Pucadyil TJ, Tewary P, Madhubala R, Chattopadhyay A. Cholesterol is required for *Leishmania donovani* infection: Implications in leishmaniasis. Mol Biochem Parasitol. 2004;133:145–52.
59. Bansal D, Bhatti HS, Sehgal R. Role of cholesterol in parasitic infections. Lipids Health Dis. 2005;4:1–7.
60. Stanley RG, Jackson CL, Griffiths K, Doenhoff MJ. Effects of *Schistosoma mansoni* worms and eggs on circulating cholesterol and liver lipids in mice. Atherosclerosis. 2009;207:131–8.
61. Rivero MR, Miras SL, Quiroga R, Rópolo AS, Touz MC. *Giardia lamblia* low-density lipoprotein receptor-related protein is involved in selective lipoprotein endocytosis and parasite replication. Mol Microbiol. 2011;79:1204–19.
62. Magen E, Bychkov V, Ginovker A, Kashuba E. Chronic *Opisthorchis felineus* infection attenuates atherosclerosis - An autopsy study. Int J Parasitol. Australian Society for Parasitology Inc.; 2013;43:819–24.
63. O'neal AJ, Butler LR, Rolandelli A, Gilk SD, Pedra JHF. Lipid hijacking: A unifying theme in vector-borne diseases. Elife. 2020;9:1–31.
64. Tokumasu F, Hayakawa EH, Fukumoto J, Tokuoka SM, Miyazaki S. Creative interior design by *Plasmodium falciparum*: Lipid metabolism and the parasite's secret chamber. Parasitol Int. Elsevier B.V.; 2021;83:102369.
65. Barrett J. Nutrition and Biosynthesis. Biochem Parasit Helminths. 1981. p. 149–239.
66. Vorel J, Cwiklinski K, Roudnický P, Ilgová J, Jedličková L, Dalton JP, et al. *Eudiplozoon nipponicum* (Monogenea, Diplozoidae) and its adaptation to haematophagy as revealed by transcriptome and secretome profiling. BMC Genomics. 2021;22:1–17.
67. Lombardo JF, Pórfido JL, Sisti MS, Giorello AN, Rodríguez S, Córsico B, et al. Function of lipid binding proteins of parasitic helminths: still a long road. Parasitol Res. 2022;121:1117–29.
68. Schrama D, Richard N, Silva TS, Figueiredo FA, Conceição LEC, Burchmore R, et al. Enhanced dietary formulation to mitigate winter thermal stress in gilthead sea bream (*Sparus aurata*): a 2D-DIGE plasma proteome study. Fish Physiol Biochem. Fish Physiology and Biochemistry; 2017;43:603–17.
69. Diógenes AF, Teixeira C, Almeida E, Skrzynska A, Costas B, Oliva-Teles A, et al. Effects of dietary tryptophan and chronic stress in gilthead seabream (*Sparus aurata*) juveniles fed corn distillers dried grains with solubles (DDGS) based diets. Aquaculture. 2019;498:396–404.
70. Benedito-Palos L, Ballester-Lozano GF, Simó P, Karalazos V, Ortiz Á, Calduch-Giner J, et al. Lasting effects of butyrate and low FM/FO diets on growth performance, blood haematology/biochemistry and molecular growth-related markers in gilthead sea bream (*Sparus aurata*). Aquaculture. 2016;454:8–18.
71. Bayly GR. Lipids and disorders of lipoprotein metabolism. In: Marshall WJ, Lapsley M, Day AP, Ayling RM, editors. Clin Biochem Metab Clin Asp. 3rd ed. 2014. p. 702–36.
72. Nelson DL, Cox MM. Lipid Biosynthesis. In: Nelson DL, Cox MM, editors. Lehninger Princ Biochem. 7th ed. 2017.

73. Han R. Plasma lipoproteins are important components of the immune system. Microbiol Immunol. 2010;54:246–53.
74. Norata GD, Pirillo A, Ammirati E, Catapano AL. Emerging role of high density lipoproteins as a player in the immune system. Atherosclerosis. 2012;220:11–21.
75. Grao-Cruces E, López-Enríquez S, Martín ME, Montserrat-de la Paz S. High-density lipoproteins and immune response: A review. Int J Biol Macromol. B.V.; 2022;195:117–23.
76. Van Der Stoep M, Korporaal SJA, Van Eck M. High-density lipoprotein as a modulator of platelet and coagulation responses. Cardiovasc Res. 2014;103:362–71.
77. Buchmann K. Antiparasitic Immune Responses. In: Buchmann K, Secombes CJ, editors. Principles of Fish Immunology, From Cells Molecules to Host Proteins. 1st ed. 2022. p. 535–63.
78. Zhou S, Li WX, Zou H, Zhang J, Wu SG, Li M, et al. Expression analysis of immune genes in goldfish (*Carassius auratus*) infected with the monogenean parasite *Gyrodactylus kobayashii*. Fish Shellfish Immunol. 2018;77:40–5.
79. Zhang C, Li DL, Chi C, Ling F, Wang GX. *Dactylogyrus intermedius* parasitism enhances *Flavobacterium columnare* invasion and alters immune-related gene expression in *Carassius auratus*. Dis Aquat Organ. 2015;116:11–21.
80. Gettins PGW. Serpin Structure, Mechanism, and Function. Chem Rev. 2002;102:4751–803.
81. Law RHP, Zhang Q, McGowan S, Buckle AM, Silverman GA, Wong W, et al. An overview of the serpin superfamily. Genome Biol. 2006;7:1–11.
82. Huntington JA. Serpin structure, function and dysfunction. J Thromb Haemost. 2011;9:26–34.
83. Sanrattana W, Maas C, de Maat S. SERPINs-From Trap to Treatment. Front Med. 2019;6:1–8.
84. Knox DP. Proteinase inhibitors and helminth parasite infection. Parasite Immunol. 2007;29:57–71.
85. Molehin AJ, Gobert GN, McManus DP. Serine protease inhibitors of parasitic helminths. Parasitology. 2012;139:681–95.
86. Bao J, Pan G, Poncz M, Wei J, Ran M, Zhou Z. Serpin functions in host-pathogen interactions. PeerJ. 2018;2018:1–16.
87. Roudnický P, Vorel J, Ilgová J, Benovics M, Norek A, Jedličková L, et al. Identification and partial characterization of a novel serpin from *Eudiplozoon nipponicum* (Monogenea, Polyopisthocotylea). Parasite. 2018;25.
88. Jedličková L, Dvořák J, Hrachovinová I, Ulrychová L, Kašný M, Mikeš L. A novel Kunitz protein with proposed dual function from *Eudiplozoon nipponicum* (Monogenea) impairs haemostasis and action of complement in vitro. Int J Parasitol. 2019;49:337–46.
89. Tirloni L, Kim TK, Berger M, Termignoni C, Da Silva Vaz I, Mulenga A. *Amblyomma americanum* serpin 27 (AAS27) is a tick salivary anti-inflammatory protein secreted into the host during feeding. PLoS Negl Trop Dis. 2019;13:1–27.
90. Hamilton S, McLean K, Monaghan SJ, McNair C, Inglis NF, McDonald H, et al. Characterisation of proteins in excretory/secretory products collected from salmon lice, *Lepeophtheirus salmonis*.

Parasites and Vectors. Parasites & Vectors; 2018;11:1–9.

91. Quezada LAL, McKerrow JH. Schistosome serine protease inhibitors: Parasite defense or homeostasis? An Acad Bras Cienc. 2011;83:663–72.
92. Molehin AJ, Gobert GN, Driguez P, McManus DP. Characterisation of a secretory serine protease inhibitor (SjB6) from *Schistosoma japonicum*. Parasites and Vectors. 2014;7:1–12.
93. Verissimo CDM, Jewhurst HL, Tikhonova IG, Urbanus RT, Maule AG, Dalton JP, et al. *Fasciola hepatica* serine protease inhibitor family (Serpins): Purposely crafted for regulating host proteases. PLoS Negl. Trop. Dis. 2020.
94. Sánchez Di Maggio L, Tirloni L, Uhl M, Carmona C, Logullo C, Mulenga A, et al. Serpins in *Fasciola hepatica*: insights into host–parasite interactions. Int J Parasitol. 2020;50:931–43.
95. Hirazawa N, Umeda N, Hatanaka A, Kuroda A. Characterization of serine proteases in the monogenean *Neobenedenia girellae*. Aquaculture. 2006;255:188–95.
96. Rao Y zhu, Yang T bao. cDNA cloning, mRNA expression and recombinant expression of a cathepsin L-like cysteine protease from *Neobenedenia melleni* (Monogenea: Capsalidae). Aquaculture. 2007;269:41–53.
97. Choi SH, Kwon SR, Lee EH, Kim KH. Molecular cloning, functional characterization and localization of an annexin from a fish gill fluke *Microcotyle sebastis* (Platyhelminthes: Monogenea). Mol Biochem Parasitol. 2009;163:48–53.
98. Jedličková L, Dvořáková H, Dvořák J, Kašný M, Ulrychová L, Vorel J, et al. Cysteine peptidases of *Eudiplozoon nipponicum*: A broad repertoire of structurally assorted cathepsins L in contrast to the scarcity of cathepsins B in an invasive species of haematophagous monogenean of common carp. Parasites and Vectors. 2018;11:1–17.
99. Pham CTN. Neutrophil serine proteases: Specific regulators of inflammation. Nat Rev Immunol. 2006;6:541–50.
100. Rau JC, Mitchell JW, Fortenberry YM, Church FC. Heparin Cofactor II: Discovery, Properties, and Role in Controlling Vascular Homeostasis. Semin Thromb Hemost. 2011;37:339–48.
101. Beinrohr L, Murray-Rust TA, Dyksterhuis L, Závodszky P, Gál P, Pike RN, et al. Serpins and the complement system. Methods Enzymol. 2011;499:55–75.
102. Rossi V, Bally I, Lacroix M, Arlaud GJ, Thielens NM. Classical complement pathway components C1r and C1s: Purification from human serum and in recombinant form and functional characterization. Methods Mol Biol. 2014;1100:43–60.
103. Mutch NJ. Regulation of fibrinolysis by platelets. 4th ed. Platelets. Elsevier Inc.; 2019.
104. Yamamoto K, Yoshida K, Miyagoe Y, Ishikawa A, Hanaoka K, Nomoto S, et al. Quantitative evaluation of expression of iron-metabolism genes in ceruloplasmin-deficient mice. Biochim Biophys Acta. 2002;1588:195–202.
105. Das S, Sahoo PK. Ceruloplasmin, a moonlighting protein in fish. Fish Shellfish Immunol. 2018;82:460–8.

106. Orzheshkovskyi V V., Trishchynska MA. Ceruloplasmin: Its Role in the Physiological and Pathological Processes. Neurophysiology. 2019;51:141–9.
107. Osikov M V., Makarov E V., Krivokhizhina L V. Ceruloplasmin prevents hemostatic disorders during experimental hyperammonemia. Bull Exp Biol Med. 2006;142:416–8.

Figures

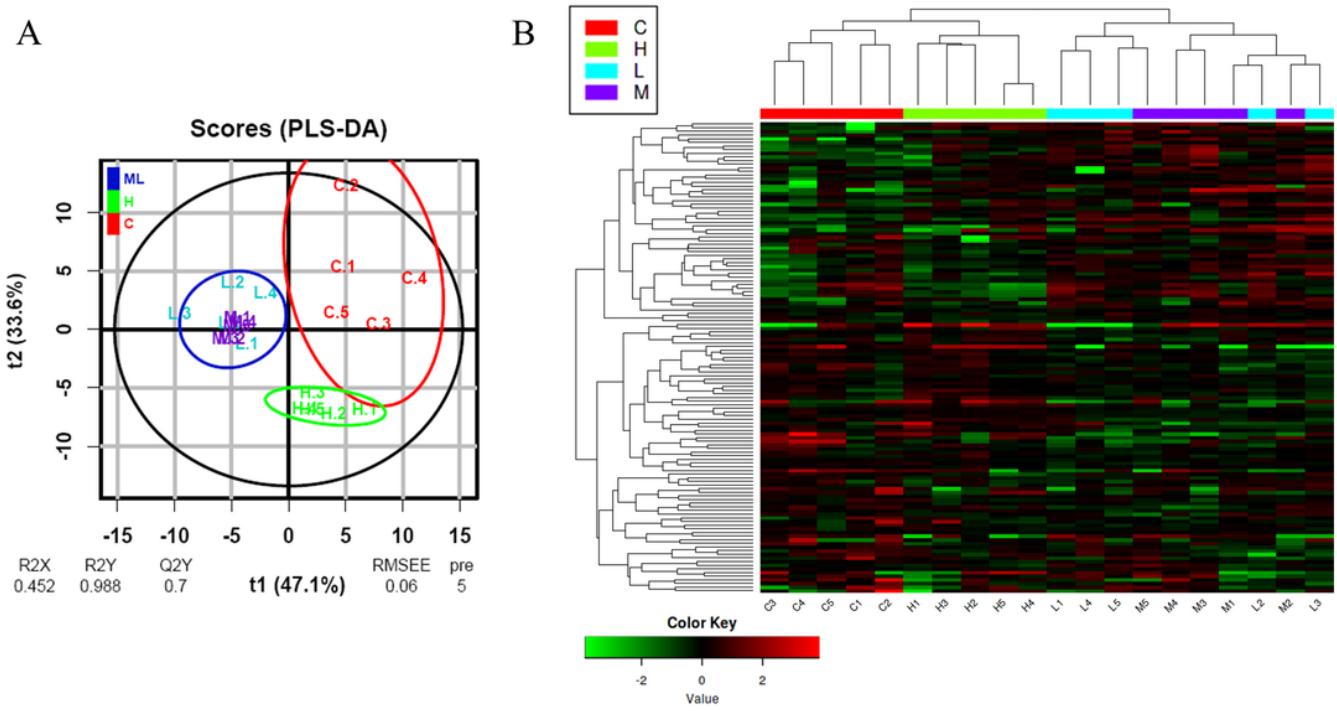

Figure 1

A) Two dimensional PLS-DA score plot representing the distribution of the samples between the first two components of the model. Control (C) uninfected fish are represented in red, *Sparicotyle chrysophrii* infected fish are represented in green, violet and blue (high (H), medium (M) and low (L) degree of infection, respectively). Ellipses represent the Mahalanobis distance. B) Heatmap representing the abundance distribution (Z-score) of the 129 proteins identified to be driving the separation among groups in A).

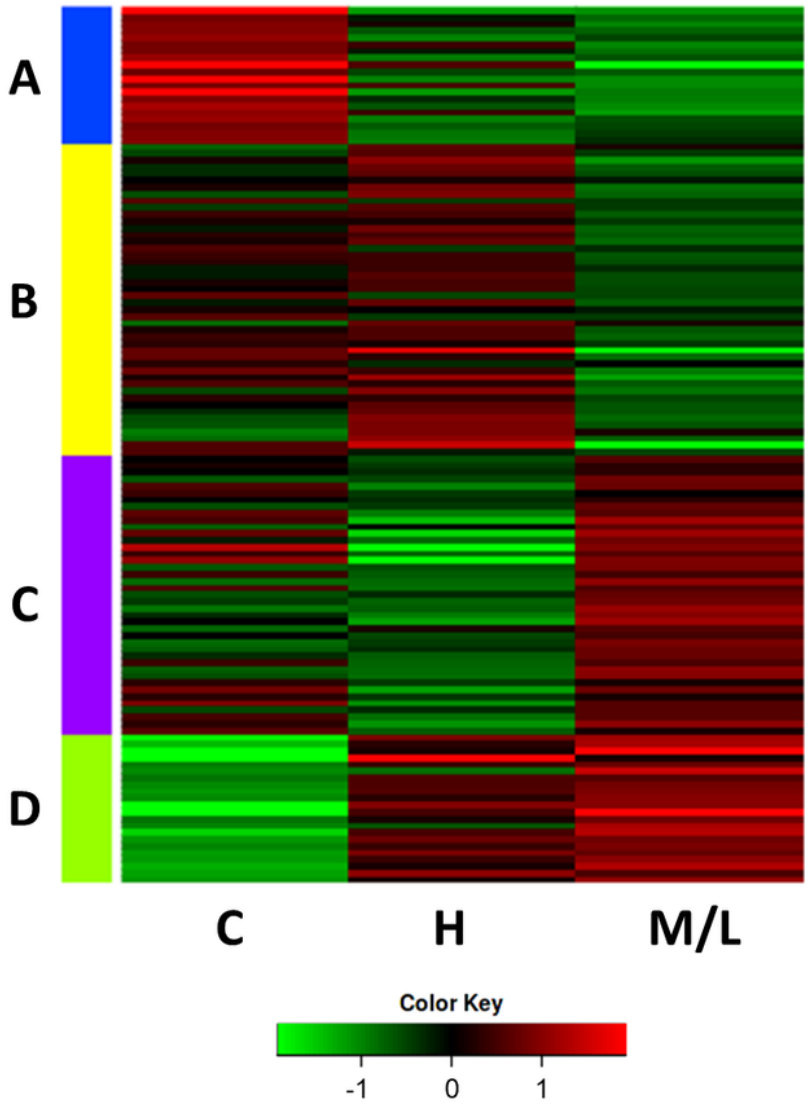

Figure 2

K-means analysis separating the 129 discriminant proteins in four clusters based on the expression level in the different groups. Different colours indicate different clusters. Cluster A: N = 20, Cluster B: N = 46, Cluster C: N = 41, Cluster D: N = 22. Group means are represented for clarity. C = control; H = high degree of infection; M/L = medium/low degree of infection.

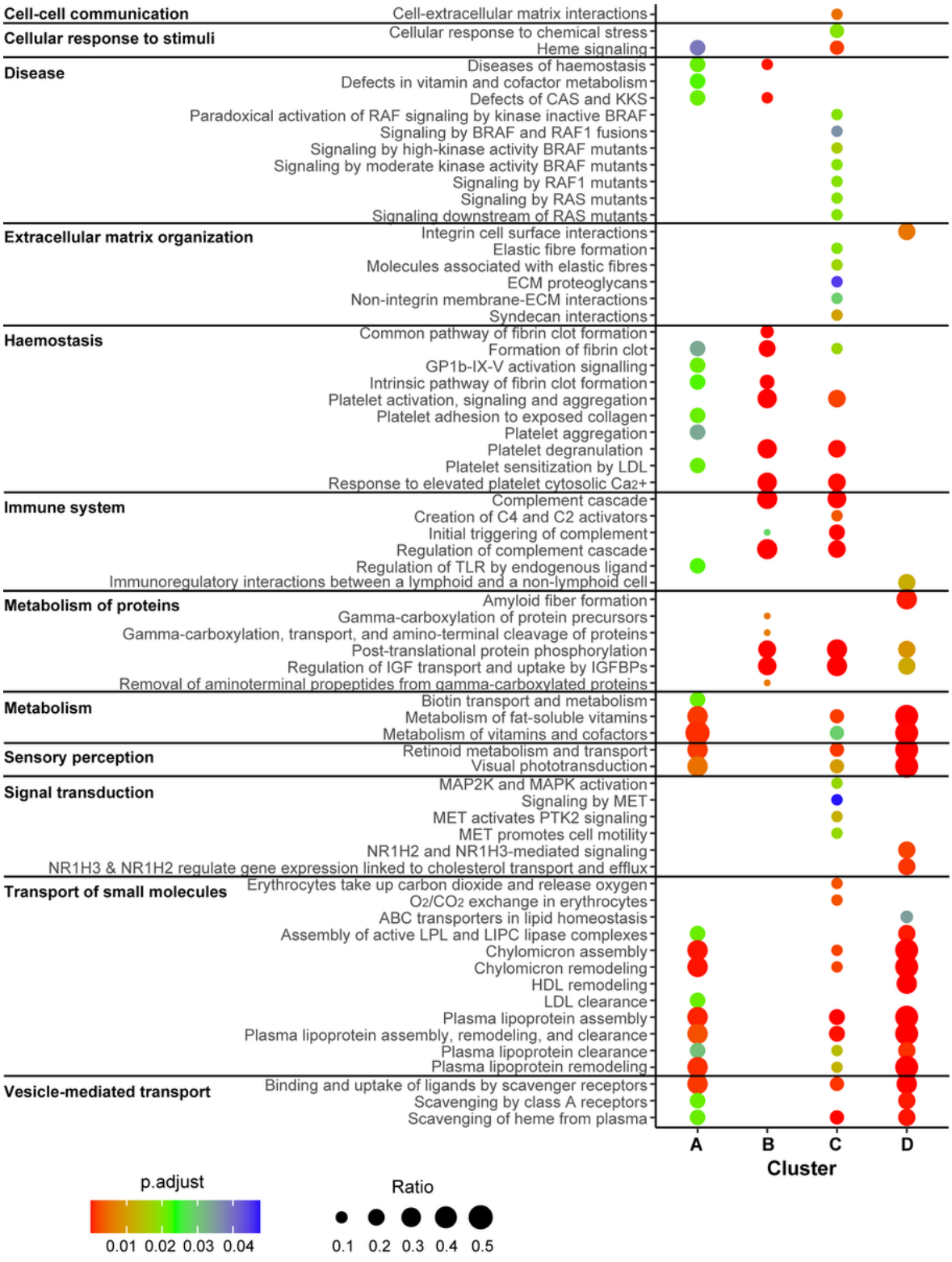

Figure 3

Dotplot pathway enrichment map showing significantly overrepresented pathways (*p.* adjust < 0.05) when considering the proteins belonging to the different k-means clusters represented in Fig. 2. The

colour of the dots represents the *p.* adjust value and the size represents the proportion of proteins relative to the total amount of proteins for each pathway.

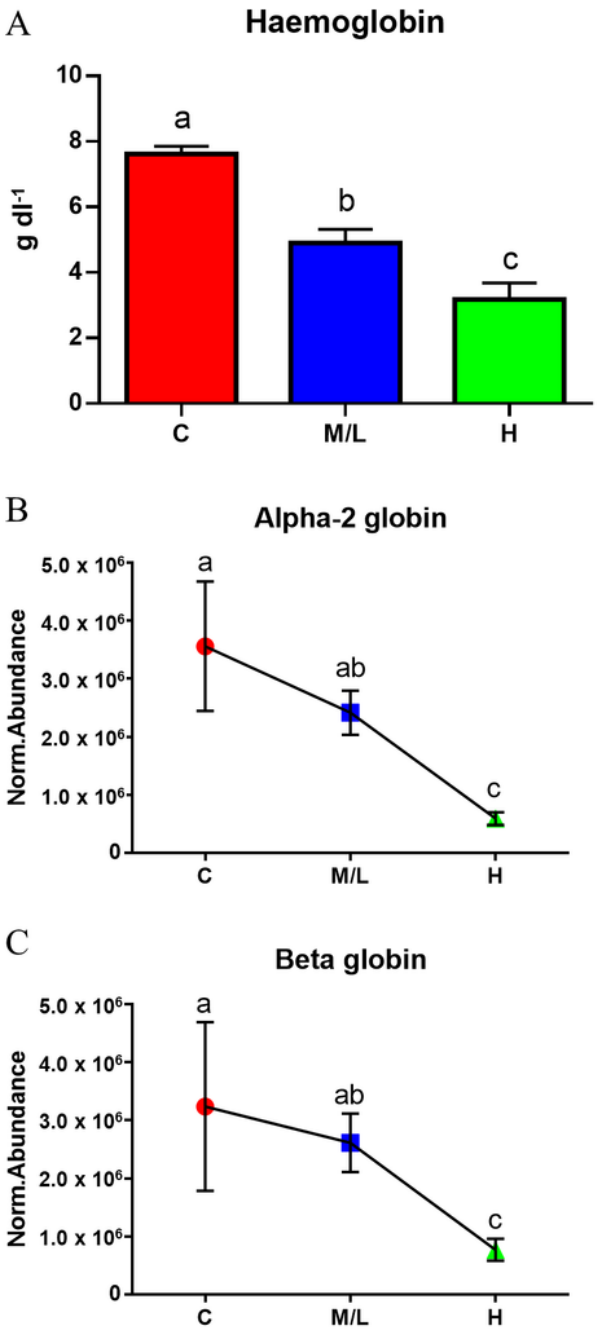

Figure 4

Haemoglobin values measured in control (C, *n* = 42) and *Sparicotyle chrysophrii* infected fish with a medium/low (M/L, *n* = 31) and high (H, *n* = 16) infection degree (A). Normalized protein abundance

values of alpha-2 globin (B) and beta-globin (C) measured by proteomics in plasma samples of control (C, *n* = 5), medium/low (M/L, *n* = 10), and high (H, *n* = 5) infection groups. Values are represented as mean ± SEM and statistical differences among groups are noted with different letters (Kruskall-Wallis test, $p < 0.05$).

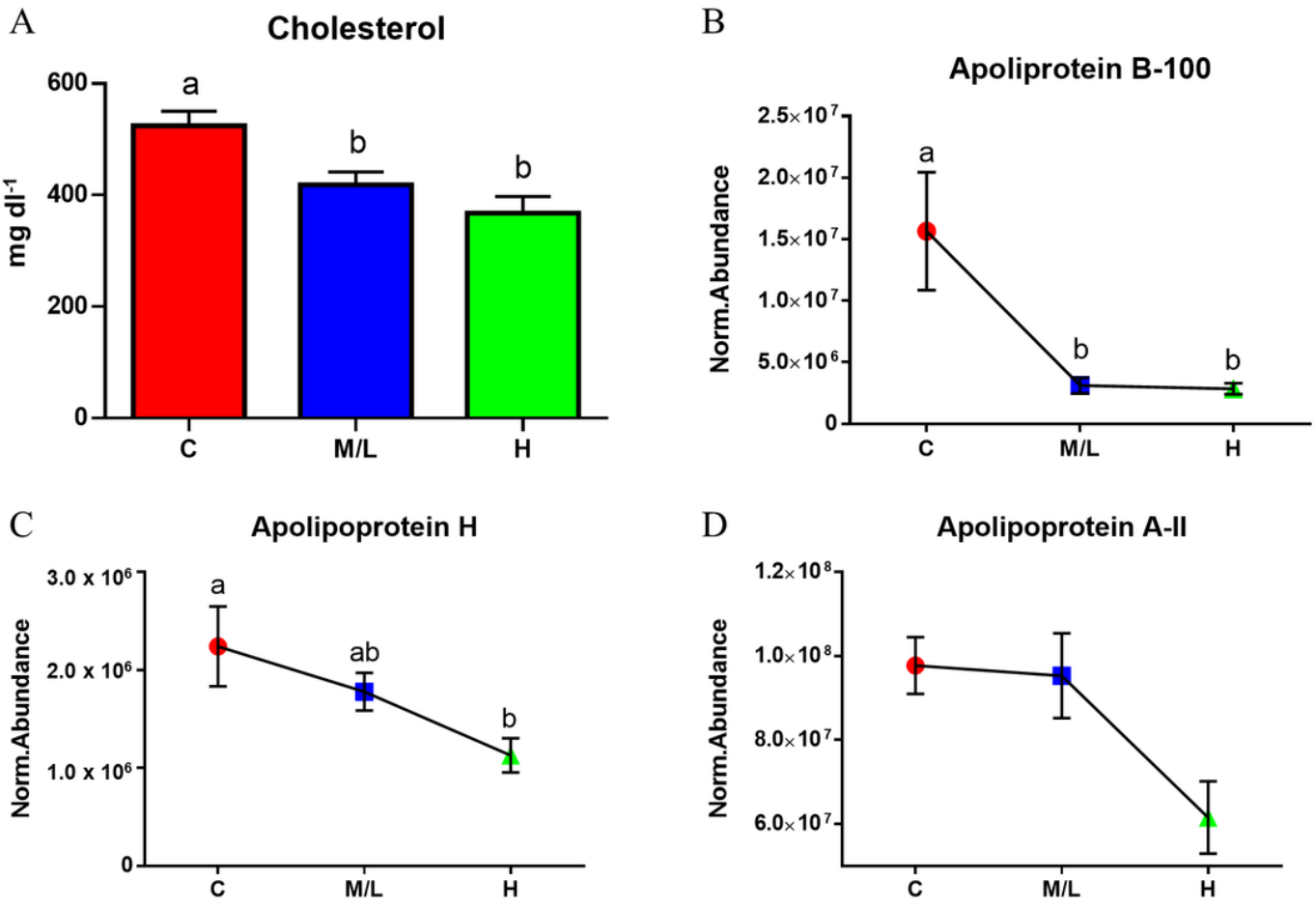

Figure 5

Plasma cholesterol values measured in control (C, *n* = 36) and *Sparicotyle chrysophrii* infected fish with a medium/low (M/L, *n* = 30) and high (H, *n* = 14) infection degree (A). Normalised protein abundance values of apolipoprotein B-100 (B), apolipoprotein H (C) and apolipoprotein A-II (D) measured by proteomics in plasma samples of control (C, *n* = 5), medium/low (M/L, *n* = 10), and high (H, *n* = 5) infection groups. Values are represented as mean ± SEM and statistical differences among groups are noted with different letters (one-way ANOVA (A, C, D) or Kruskall-Wallis test (B), $p < 0.05$).

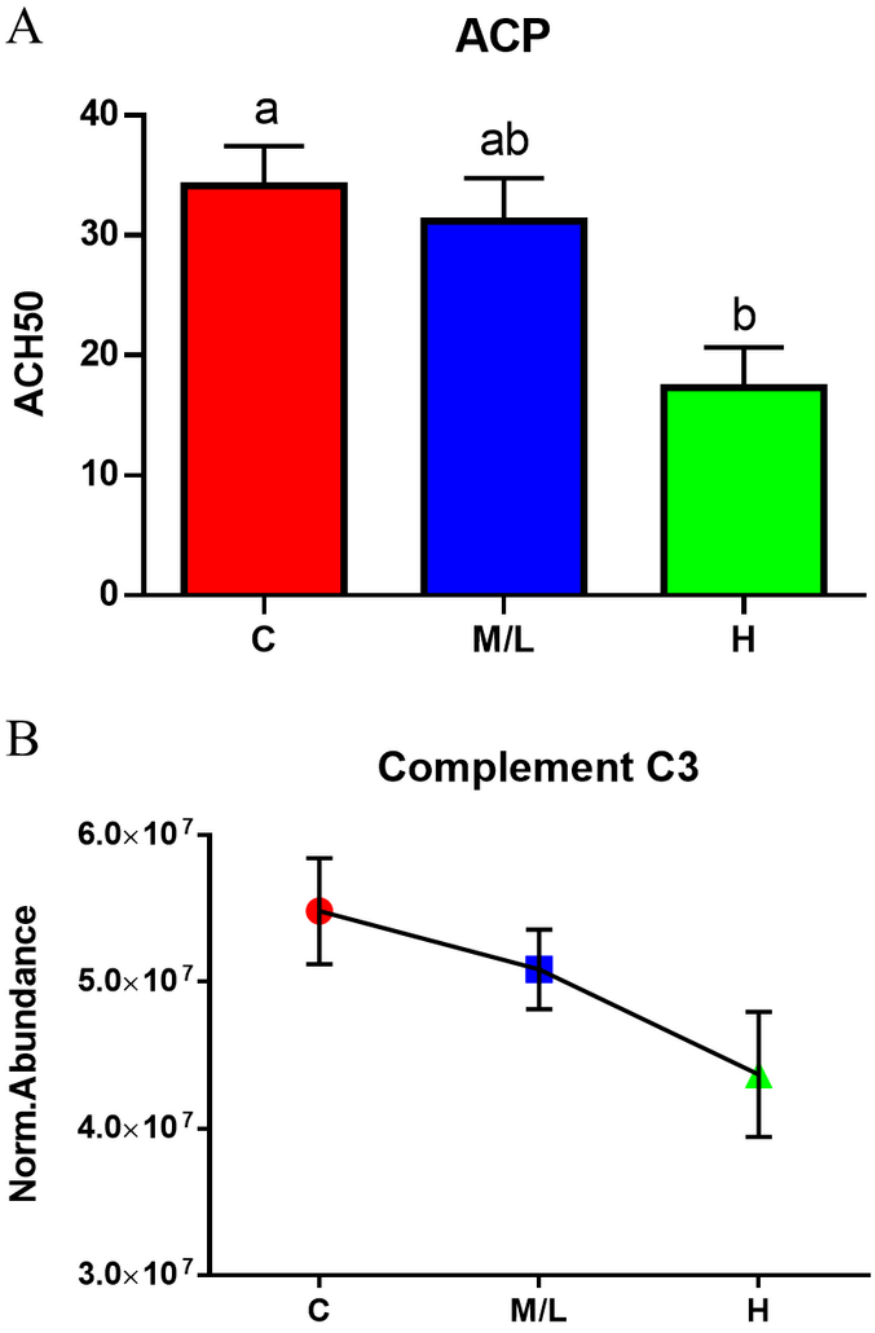

Figure 6

Activity of plasma alternative complement pathway (ACP) measured in control (C, *n* = 41) and *Sparicotyle chrysophrii* infected fish with a medium/low (M/L, *n* = 33) and high (H, *n* = 13) infection degree (A). Normalized protein abundance values of complement C3 protein (B) measured by proteomics in plasma samples of control (C, *n* = 5), medium/low (M/L, *n* = 10), and high (H, *n* = 5) infection groups. Values are

represented as mean ± SEM and statistical differences among groups are noted with different letters (one-way ANOVA, $p < 0.05$).

Supplementary Files

This is a list of supplementary files associated with this preprint. Click to download.

- Additionalfile1.pdf
- Additionalfile2.xlsx
- Additionalfile3.pdf
- GraphicalAbstract.tif